ACCOUNTS of chemical research

Article

pubs.acs.org/accounts

Noble Metal Aerogels—Synthesis, Characterization, and Application as Electrocatalysts

Wei Liu,[†] Anne-Kristin Herrmann,[†] Nadja C. Bigall,[‡] Paramaconi Rodriguez,[∥] Dan Wen,[†] Mehtap Oezaslan,[§,#] Thomas J. Schmidt,[§,⊥] Nikolai Gaponik,[†] and Alexander Eychmüller*,[†]

[†]Physical Chemistry and Center for Advancing Electronics Dresden, TU Dresden, Bergstraße 66b, D-01069 Dresden, Germany

[‡]Institute of Physical Chemistry and Electrochemistry, Leibniz Universität Hannover, Callinstraße 3A, D-30167 Hanover, Germany

[§]Electrochemistry Laboratory, Paul Scherrer Institute, CH-5232 Villigen PSI, Switzerland

[∥]School of Chemistry, The University of Birmingham, Birmingham B15 2TT, United Kingdom

[⊥]Laboratorium für Physikalische Chemie, ETH Zürich, Vladimir-Prelog-Weg 2, CH-8093 Zürich, Switzerland

Supporting Information

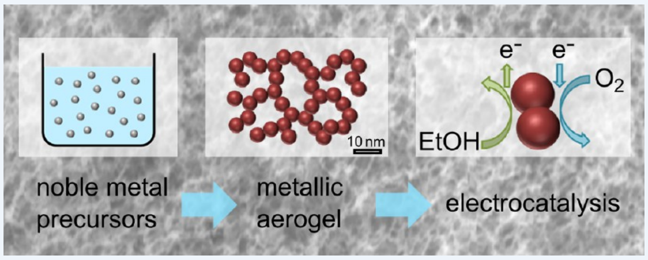

CONSPECTUS: Metallic and catalytically active materials with high surface area and large porosity are a long-desired goal in both industry and academia. In this Account, we summarize the strategies for making a variety of self-supported noble metal aerogels consisting of extended metal backbone nanonetworks. We discuss their outstanding physical and chemical properties, including their three-dimensional network structure, the simple control over their composition, their large specific surface area, and their hierarchical porosity. Additionally, we show some initial results on their excellent performance as electrocatalysts combining both high catalytic activity and high durability for fuel cell reactions such as ethanol oxidation and the oxygen reduction reaction (ORR). Finally, we give some hints on the future challenges in the research area of metal aerogels. We believe that metal aerogels are a new, promising class of electrocatalysts for polymer electrolyte fuel cells (PEFCs) and will also open great opportunities for other electrochemical energy systems, catalysis, and sensors.

The commercialization of PEFCs encounters three critical obstacles, viz., high cost, insufficient activity, and inadequate long-term durability. Besides others, the sluggish kinetics of the ORR and alcohol oxidation and insufficient catalyst stability are important reasons for these obstacles. Various approaches have been taken to overcome these obstacles, e.g., by controlling the catalyst particle size in an optimized range, forming multimetallic catalysts, controlling the surface compositions, shaping the catalysts into nanocrystals, and designing supportless catalysts with extended surfaces such as nanostructured thin films, nanotubes, and porous nanostructures. These efforts have produced plenty of excellent electrocatalysts, but the development of multisynergetic functional catalysts exhibiting low cost, high activity, and high durability still faces great challenges.

In this Account, we demonstrate that the sol–gel process represents a powerful "bottom-up" strategy for creating nanostructured materials that tackles the problems mentioned above. Aerogels are unique solid materials with ultralow densities, large open pores, and ultimately high inner surface areas. They magnify the specific properties of nanomaterials to the macroscale via self-assembly, which endow them with superior properties. Despite numerous investigations of metal oxide aerogels, the investigation of metal aerogels is in the early stage. Recently, aerogels including Fe, Co, Ni, Sn, and Cu have been obtained by nanosmelting of hybrid polymer–metal oxide aerogels. We report here exclusively on mono-, bi- and multimetallic noble metal aerogels consisting of Ag, Au, Pt, and Pd and their application as electrocatalysts.

INTRODUCTION

Aerogels are unique solid materials with extremely low densities, high porosity, and large inner surface area.[1] They combine the chemical and physical properties of nanomaterials with those of the macroscale and may integrate the specific properties of the various constituents in one resulting material, making aerogels very attractive in various applications such as catalysis, thermoresistors, piezoelectrics, and sensors. The first aerogels (silica and alike) were pioneered by Kistler in 1931.[2] Since then, the research on aerogels has largely widened to include inorganic (e.g., metal oxide, carbide, silica–metal oxide, and metal-doped), inorganic–organic hybrid (e.g., polymer-cross-linked inorganic aerogels), organic (e.g., all major polymeric classes, including resorcinol/formaldehyde, melamine/formaldehyde, polyurethane, polyamide, polyurea, polynorbornene, polydicyclopentadiene, conducting polymers (polythiophene) and polybenzoxazine), and carbon aerogels.[1,3−5] Recently, a major breakthrough in the development of inorganic aerogels such as metal sulfides, selenides, and

Received: June 27, 2014
Published: January 22, 2015

ACS Publications

DOI: 10.1021/ar500237c
Acc. Chem. Res. 2015, 48, 154−162

tellurides (i.e., chalcogenide semiconductors) was made by Brock, Kanatzidis, and their co-workers.[6−8] More recently, an important step forward toward metallic aerogels was achieved by Leventis and co-workers, who obtained metallic aerogels including Fe, Co, Ni, Sn, and Cu by nanosmelting of hybrid carbonizable polymer−metal oxide aerogels.[4,9−13] However, the extension of this method to metals that cannot be carbothermally reduced from their oxides remains a challenge.[14] Even though metal-doped oxide/carbon-based aerogels such as SiO_2, Al_2O_3, TiO_2, and carbon aerogels doped with Pt, Pd, Au, and Cu have been realized by impregnation or by the sol−gel method for a long time,[3,15,16] the fabrication of pure metallic aerogels with metal backbones by the direct sol−gel method has very recently been achieved for the first time, as will be outlined below.[17−23]

Polymer electrolyte fuel cells (PEFCs) have attracted worldwide attention because of their high energy efficiency and outstanding environmental compatibility. However, the commercialization of PEFCs still faces three critical obstacles: high cost, insufficient activity, and inadequate long-term durability. Various approaches have been taken to overcome these issues by tailoring the size, composition, shape, and structure of the catalyst.[24−33] The design of supportless catalysts with extended surfaces, such as nanostructured films, nanowires, nanotubes, and porous nanostructures, has provided tremendous opportunities to improve the catalytic performance and durability. The advantages are their high surface area, large porosity, elimination of support corrosion, and high robustness.[26,30,31] In this context, a very promising class of unsupported catalyst materials are metal aerogels consisting of extended metal backbone nanonetworks. They combine the unique properties of metals (such as good electrical and thermal conductivity, catalytic activity, and ductility/malleability) with the unique properties of common aerogels (high surface area, ultralow density, and high porosity).

In this Account, we describe the recent progress in the design of noble metal aerogels together with their applications as electrocatalysts for fuel cells. After an introduction of the synthetic strategies, the main characteristics of these aerogels are discussed along with various characterizations. Before a final overview of metal aerogels, including current challenges and future prospects in this area, the first applications of noble metal aerogels as electrocatalysts with promising results for ethanol oxidation and the oxygen reduction reaction (ORR) are presented.

■ PREPARATION OF NOBLE METAL AEROGELS WITH HIGH SURFACE AREA AND POROSITY

An overview of the representative preparative strategies for noble metal aerogels via the sol−gel process is shown in Scheme 1. The formation of the hydrogel is the critical step for the preparation. To date, this has been realized via two strategies: via gelation of preformed noble metal nanoparticles (NPs) (Scheme 1, strategy (I)) or via an in situ spontaneous gelation process (Scheme 1, strategy (II)).

In the first strategy to be outlined here (Scheme 1, strategy (I)), citrate-capped monometallic NPs are first synthesized via reduction of the noble metal precursor ($HAuCl_4$, $AgNO_3$, H_2PtCl_6, or $PdCl_2$) with $NaBH_4$ using trisodium citrate as a stabilizer.[17,21] The diameters of the obtained Au, Pt, and Pd NPs are 3−5, 3−6, and 3−6 nm, respectively, and the Ag NPs exhibit a bimodal size distribution with diameters in the range of 3−6 and 8−15 nm. Other recently published routes lead to hollow preformed bimetallic "nanoshell" particles via the galvanic displacement reaction between citrate-stabilized Ag NPs and noble metal precursors such as $HAuCl_4$, K_2PdCl_4, and K_2PtCl_4 or to thiolate-coated Ag nanoshell particles via fast chemical reduction of preformed Ag_2O NPs.[22,23] Citrate is frequently selected as a stabilizer since it can endow both electrostatic and steric repulsions to the metal NPs.[34] Moreover, the coordination interaction between the citrate anions and the metal NP surface is relatively weak.[34] Gelation of the preformed noble metal NP solutions or their mixtures is induced by deliberate destabilization via the following typical steps. First of all, the solution is concentrated by a factor of 10−50 with polystyrene centrifuge filters or a rotary evaporator. During the filter concentration, water washing is carried out to minimize the concentration of residual stabilizer and impurities. Then the gelation can be induced by settling of the concentrated NP solutions at room or increased temperature (323−348 K) or via addition of destabilizers such as ethanol, H_2O_2, etc. By means of strategy (I), a wide range of monometallic hydrogels, including Au, Ag, Pt, and Pd, and multimetallic hydrogels, including Au−Ag, Au−Pd, Pt−Ag, Pd−Ag, Pt−Pd, Au−Ag−Pt, Au−Pt−Pd, Ag−Pt−Pd, and Au−Ag−Pt−Pd, have been prepared.[17,21]

Scheme 1. Schematic Illustration of Noble Metal Aerogel Preparation via Gelation of Preformed Nanoparticles (Strategy (I)) and via an in Situ Spontaneous Gelation Process (Strategy (II))

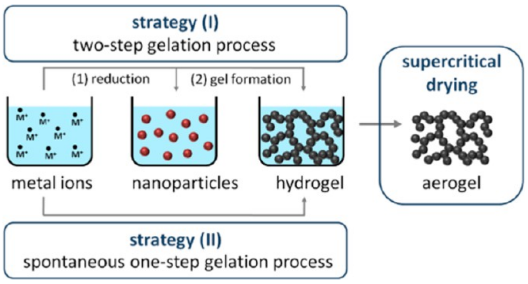

In the second strategy (Scheme 1, strategy (II)), the hydrogels are spontaneously formed from the in situ reduction of noble metal precursors with $NaBH_4$ in a single step, i.e., without the preformation of adequately stabilized NPs.[18−20] To date, α,β,γ-cyclodextrin (CD)-protected Pd ($Pd_{\alpha,\beta,\gamma\text{-CD}}$) hydrogels,[18] pure Pd and Pt hydrogels, and bimetallic Pt_nPd_{100-n} hydrogels with controllable Pt to Pd ratios[19,20] have been obtained by this approach. As demonstrated by the transmission electron microscopy (TEM) images in Figure S1 in the Supporting Information, this hydrogel formation continuously proceeds via spontaneous assembly involving four main continuous stages from the transient formation of NPs, via short nanowires, nanowire networks, and finally to the hydrogels. The salts generated during the synthesis are suspected to play an important role in the gel formation. They increase the ionic strength of the solution and decrease the electrostatic repulsion between the primary NPs; they may also transform the isotropic electrostatic repulsions between the NPs into anisotropic forms, thus leading to the rapid anisotropic agglomeration/assembly of the non-further-stabilized NPs.[18]

Direct evaporation of the liquid from a wet gel can lead to considerable shrinkage and even collapse of the network structure of the hydrogel due to the high surface tension or capillary pressure generated during the drying processes.

Supercritical drying is an appropriate way to retain the internal structure of the hydrogel also in the dry state. It prevents a direct phase transition of the solvent from the liquid to the gas phase, minimizes the forces leading to the collapse of the fragile pores inside the structure, and allows the gel to be dried with very little shrinkage. Consequently, the resulting aerogels have a higher surface area, an intact pore shape, and a larger pore volume than those porous structures obtained using conventional drying methods. Thus, CO_2 supercritical drying is utilized throughout to transform the noble metal hydrogels to aerogels. Before supercritical drying, the water in the pores of the hydrogels is replaced by acetone and further with liquid CO_2.

■ CHARACTERIZATIONS

Morphology

TEM and scanning electron microscopy (SEM) were utilized for the morphological characterization of the noble metal aerogels prepared by both synthetic routes shown in Scheme 1. Some representative images are shown in Figures 1 and 2. All of the aerogels (no matter whether mono- or multimetallic or prepared via either of the strategies outlined above) show three-dimensional-network-like structures with extended nanochains interconnected with each other together with a large number of open pores and tunnels.[17−21] Depending on the nature of the noble metal NPs, the nanochains may appear in the form of fused-nanowire-like structures or necklacelike chains, as shown in Figure 2 and in Figures S2−S4 and the detailed information in the Supporting Information.[17−21]

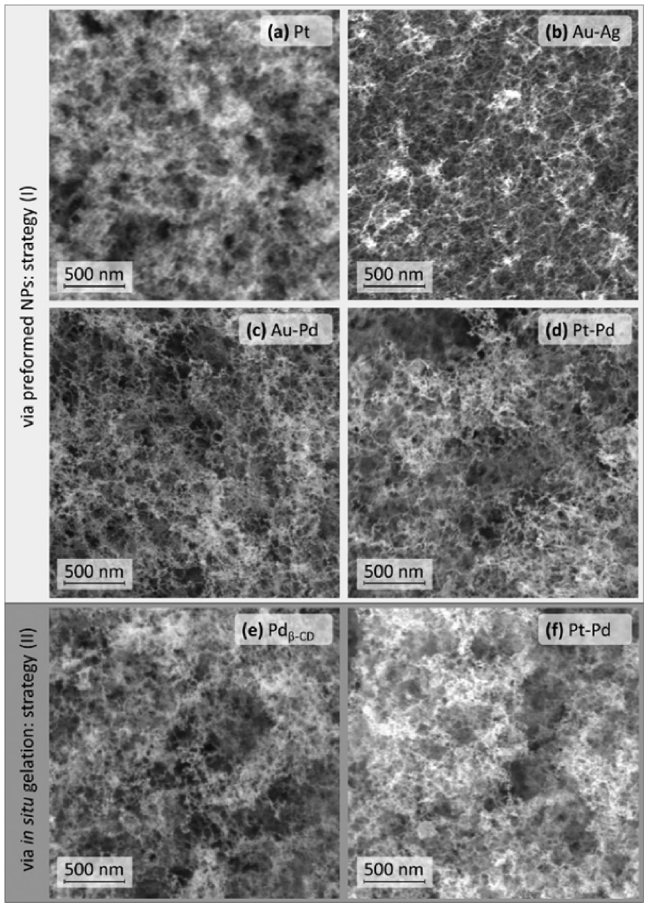

Figure 1. SEM images of some representative noble metal aerogels. The aerogels in (a−d) were prepared via strategy (I); the aerogels in (e) and (f) were obtained by strategy (II). The images in (c) and (d) are reproduced from ref 21. Copyright 2014 American Chemical Society. The image in (e) is reproduced with permission from ref 18. Copyright 2012 Wiley-VCH Verlag GmbH & Co. KGaA, Weinheim.

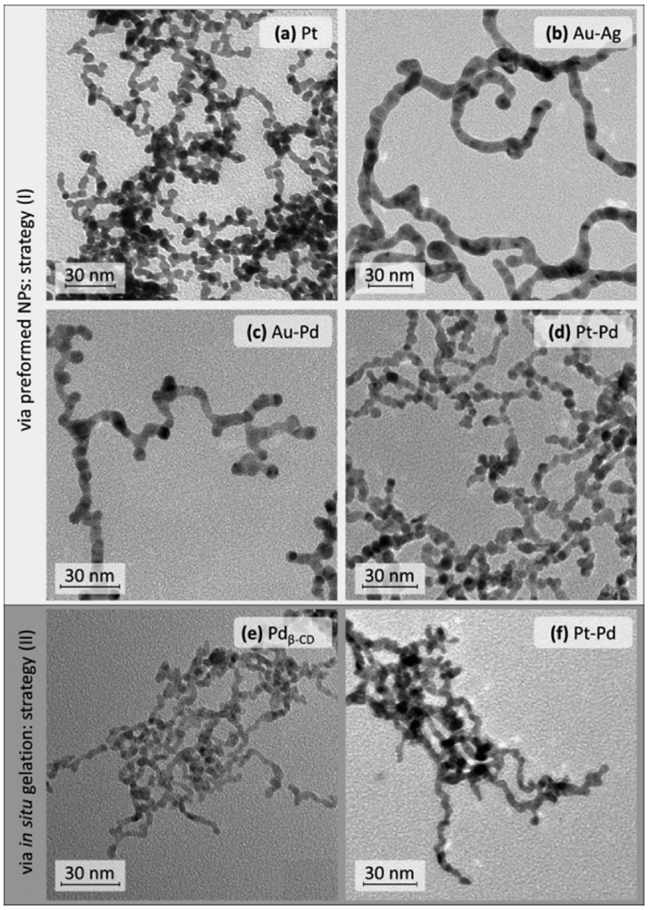

Figure 2. TEM images of a variety of noble metal aerogels. The aerogels in (a−d) were prepared via strategy (I); those in (e) and (f) were obtained via strategy (II). The images in (c) and (d) are reproduced from ref 21. Copyright 2014 American Chemical Society. The images in (e) and (f) are reproduced with permission from refs 18 and 19. Copyright 2012 and 2013 Wiley-VCH Verlag GmbH & Co. KGaA, Weinheim.

Crystalline Structure and Alloying

The crystalline structure and spatial elemental distribution of the aerogels have been investigated by high-resolution TEM (HRTEM), powder X-ray diffraction (XRD), and high-angle annular dark-field scanning transmission electron microscopy (HAADF-STEM) combined with energy-dispersive X-ray spectrometry (EDX). All of the noble metal aerogels show a face-centered-cubic (fcc) polycrystalline structure, as reflected by the HRTEM images and corresponding fast Fourier transform results in Figure 3 as well as the XRD patterns in Figure 4. The HRTEM images in Figure 3 also show the wide exposure of lattice planes such as the (111) plane and the existence of lattice boundaries and stacking faults along the interconnected network nanowires in the aerogels.

For multimetallic structures, the state of alloying is an important feature regarding physical properties, chemical reactivity, and catalytic activity. For the bimetallic aerogels

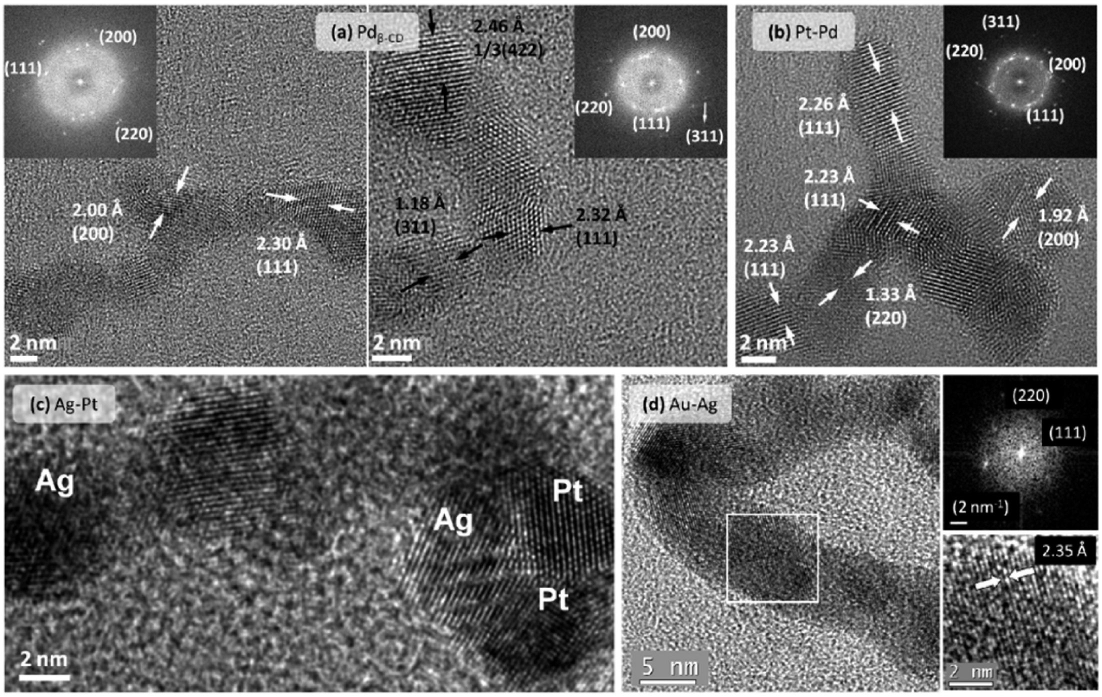

Figure 3. HRTEM images of some noble metal aerogels. Au–Ag and Ag–Pt aerogels were prepared via strategy (I). Pd$_{\beta\text{-CD}}$ and Pt–Pd aerogels were obtained via strategy (II). The images in (a) and (b) are adapted with permission from refs 18 and 19 and those in (c) and (d) from ref 17. Copyright 2012, 2013, and 2009 Wiley-VCH Verlag GmbH & Co. KGaA, Weinheim.

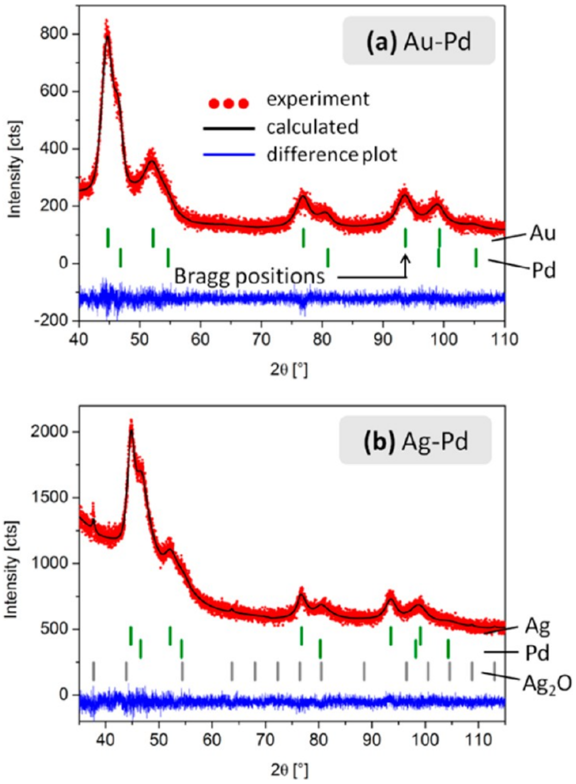

Figure 4. XRD patterns of Au–Pd and Ag–Pd aerogels synthesized via strategy (I). Adapted from ref 21. Copyright 2014 American Chemical Society.

fabricated via strategy (I), the initial building blocks of the gel structure are separated NPs of different metals. This raises the question of whether interdiffusion of the two types of metal atoms and thus alloying occur under the given conditions or the metals exist in separated phases within the structure. When the bimetallic aerogel is composed of metals of sufficiently different lattice parameters, it is relatively easy to confirm their alloying state by HRTEM and XRD. For example, the Pt–Ag aerogel evolved from preformed Pt and Ag NPs shows the morphology of the as-synthesized nanocrystals without further alloying or growth of secondary particles (Figure 3c). The two sorts of particles can be distinguished by HRTEM because of the relatively large difference in their (111) lattice spacings (2.36 Å for silver and 2.26 Å for platinum). In other examples, the powder XRD patterns of Ag–Pd and Au–Pd aerogels (Figure 4) ((111) lattice spacings of 2.35 Å for gold and 2.23 Å for palladium) clearly show separated silver/gold and palladium phases, as indicated by the two sets of patterns for silver/gold and palladium in the aerogels and especially evidenced by the well-separated reflections at $2\theta > 70°$. For bimetallic aerogels composed of metals of very similar lattice parameters, such as Au–Ag and Pt–Pd, it is very difficult to distinguish the distribution of the two metals in the aerogels by HRTEM and XRD. The common fcc crystal structure, the very similar crystallographic parameters, and the small crystallite sizes complicate the analysis. In this case, the HAADF-STEM technique combined with EDX is very useful to reveal the spatial distribution of metals in the bimetallic aerogels. For instance, the HAADF-STEM–EDX results for the Au–Ag aerogel in Figure 5 show no distinct Z contrast ($Z = 47$ for Ag and $Z = 79$ for Au) in the HAADF image, and an overall distribution of both metals along the nanochains. Hence, it is concluded from these results that interdiffusion of the gold and silver atoms between the initially monometallic NPs and therefore the formation of an alloy occurred during the network formation.

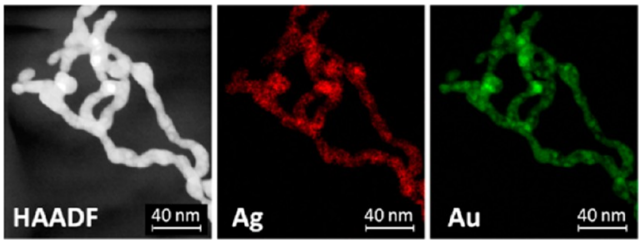

Figure 5. Phase analysis of Au–Ag aerogel using HAADF-STEM and STEM-EDX mapping of silver and gold. No pronounced Z contrast inside the nanochains is visible; the elemental mapping shows an overall distribution of both metals. Reproduced from ref 21. Copyright 2014 American Chemical Society.

Surface Area and Porosity

The porosity and surface area of the aerogels have been evaluated by nitrogen physisorption measurements. The isotherms for N_2 adsorption and desorption of the noble metal aerogels obtained to date cannot be assigned to any standard isotherms but mainly show a combination of IUPAC type-II and type-IV isotherms (Figure 6). The isotherms display multilayer adsorption behavior, and no plateau appears for high relative pressures; these characteristics indicate that the materials are mostly macroporous. The surface areas of the aerogels were determined via analysis of the isotherms by the Brunauer–Emmett–Teller (BET) method. The BET surface areas of the noble metal aerogels are in the range of 32–168 $m^2\ g_{aerogel}^{-1}$. From the comparison of the BET surface areas of porous noble metals prepared via different routes obtained from the literature (Table S1 in the Supporting Information), it is obvious that noble metal aerogels show exceptionally high surface areas. The bimetallic Pt–Pd aerogels synthesized via strategy (II) have lower surface areas than the pure Pd or Pt aerogel, which is probably due to the obvious gel volume shrinkage of the bimetallic aerogels during the acetone exchange step before supercritical drying, the lower atomic weight of Pd compared with Pt, and the smaller average diameter of the nanochain in the Pt aerogel (~2.7 nm) compared with other aerogels (~4.2 nm).

The pore size distributions and cumulative pore volumes were calculated from the desorption branch of the isotherms using the Barrett–Joyner–Halenda (BJH) theory or density functional theory, depending on the carbon content. The results together with the SEM and TEM characterizations show wide pore size distributions in the aerogels ranging from micropores to mesopores and macropores, with most of the pore volume stemming from macropores. This hierarchical pore system is of great advantage for minimizing diffusion barriers in sensor and/or catalytic applications since the diffusion rates through 10–50 nm pores are similar to those of molecules in open media.[35]

Some photographs of the noble metal aerogel monoliths are shown in Figure S5 in the Supporting Information. The monolith densities of the noble metal aerogels were estimated by weighing several monoliths and assessing their spatial dimensions. The monolith densities of the as-prepared aerogels are in the range of 0.01–0.10 g cm^{-3}, which corresponds to approximately $^1/_{1000}$ to $^1/_{120}$ of the bulk density of the respective metal(s).

Processability and Electrical Conductivity

The desired handling and/or technological integration of the fragile, porous, and irregular-shaped aerogel monoliths into device architectures is crucial for applications but remains challenging. We tried to improve the processability of the metallic gels by grafting them to several kinds of substrates.[21] By immersion of the substrates into a hydrogel solution and evaporation of the solvent, metallic xerogel films with thicknesses of several micrometers on these substrates can be obtained (Figure S6a in the Supporting Information). Even after noncritical drying, the structure shows high porosity and an open pore system. Another method to increase the processability is the formation of gel–polymer hybrid materials.[5,21,36,37] To realize this, the pores are first infiltrated with a monomer solution, and this is followed by a polymerization reaction inside the gel network structure. For

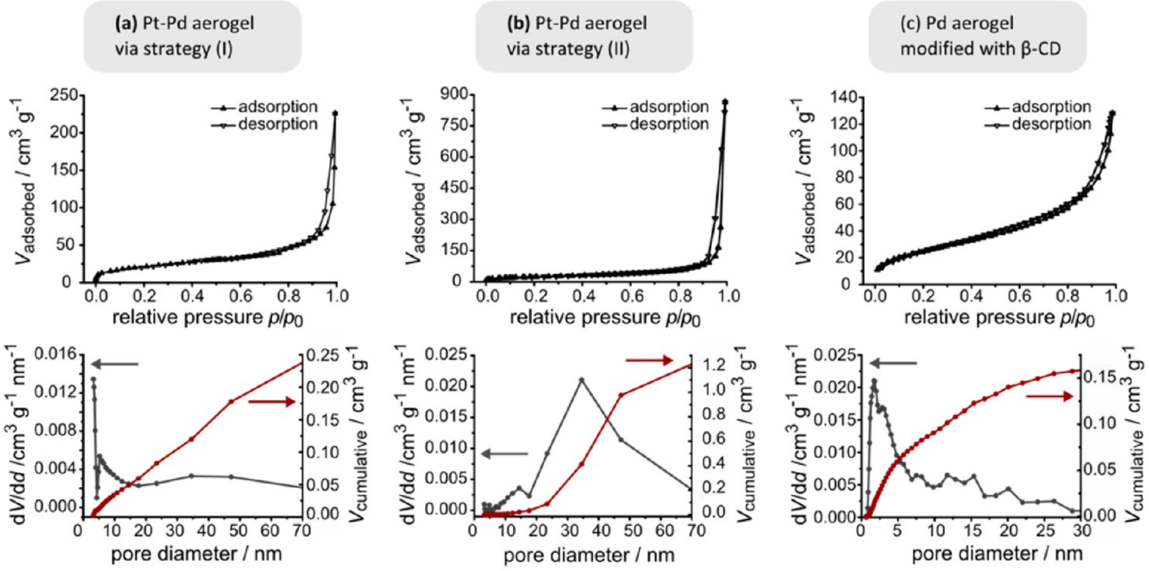

Figure 6. Nitrogen physisorption isotherms, pore size distributions, and cumulative pore volumes ($V_{cumulative}$) of (a, b) Pt–Pd aerogels prepared via strategies (I) and (II), respectively, and (c) the $Pd_{\beta\text{-CD}}$ aerogel prepared via strategy (II).

instance, a Au–Ag–Pt–poly(ethyl cyanoacrylate) hybrid gel has been obtained via this method (Figure S6b).[21]

The electrical conductivity, which is related to the electrical accessibility of the functional sites, is another important property of an electrocatalyst. The electrical conductivities of the noble metal xerogel films were measured with a van der Pauw setup (see the inset in Figure S6a).[21,38] When the layer resistance and film thickness were taken into account, specific resistances of ca. 2 Ω·mm^2/m and 5 Ω·mm^2/m were obtained for Au–Pd and Pt–Pd xerogel films on glass substrates, respectively. These values are only 2 orders of magnitude higher than those for the corresponding bulk metals, underlining the high electrical conductivity of the multimetallic nanostructures obtained by our approaches.

■ APPLICATIONS IN ELECTROCATALYSIS

As a new, unique class of materials that present high specific surface areas and large open pores, noble metal aerogels are very promising in various applications such as in heterogeneous gas-phase catalysis, electrocatalysis, and sensors. For these applications, a number of characteristics are especially favorable: (1) the hierarchical porous structures give these materials a very high specific surface area, allow efficient mass transport through the pores, and have less diffusional resistance and easier access to active sites (such as defects, facets, and left stabilizer species[18,28,29]),[39] all of which enhance the catalytic activity; (2) the aerogel networks are mostly composed of interconnected nanochains that are several nanometers in size, which is in the optimal range for electrocatalysis of processes such as the ORR (high mass activity);[24,25] and (3) the interconnected nanochains in the networks are mostly fused-nanowire-like structures with extended surfaces, which are expected to have higher durability during (electro)-catalysis.[26,30,31] Furthermore, the self-supporting character of the aerogels may prevent the loss of durability observed in conventional noble metal catalysts supported on carbon due to corrosion. Last but not least, the molar ratio of the constituent elements in the multimetallic aerogels can be controlled precisely, which allows the design of the optimum balance among composition, reactivity, durability, and cost and fully exploits the synergistic effects in enhancing the catalytic activity.[40,41]

The electrocatalytic performance of the $\mathrm{Pd}_{\alpha,\beta,\gamma\text{-CD}}$ aerogels toward ethanol oxidation was evaluated by cyclic voltammetry and chronoamperometry and compared with that of commercial Pd/C (10 wt %) (Figure 7b,c).[18] All of the $\mathrm{Pd}_{\mathrm{CD}}$ aerogels and the Pd/C electrodes show two well-defined current peaks characteristic of the electrooxidation of ethanol (Figure 7b). The mass-specific current densities (in A $\mathrm{mg_{metal}}^{-1}$) in the forward scan for the $\mathrm{Pd}_{\mathrm{CD}}$ aerogels, especially the $\mathrm{Pd}_{\alpha\text{-CD}}$ and $\mathrm{Pd}_{\beta\text{-CD}}$ aerogels, are much higher than that for the commercial Pd/C. The onset potentials of the $\mathrm{Pd}_{\alpha\text{-CD}}$, $\mathrm{Pd}_{\beta\text{-CD}}$, and $\mathrm{Pd}_{\gamma\text{-CD}}$ aerogels show negative shifts of 47–69 mV relative to that of the Pd/C electrode, implying enhanced kinetics of the ethanol electrooxidation for the $\mathrm{Pd}_{\mathrm{CD}}$ aerogels. The long-term stabilities of the $\mathrm{Pd}_{\mathrm{CD}}$ aerogels and the Pd/C electrodes were investigated by chronoamperometry (Figure 7c). The $\mathrm{Pd}_{\mathrm{CD}}$ aerogels, especially the $\mathrm{Pd}_{\alpha\text{-CD}}$ and $\mathrm{Pd}_{\beta\text{-CD}}$ aerogels, exhibit much higher initial polarization mass-specific current densities (2.8 and 2.0 times that of Pd/C, respectively), slower current decays, and higher steady-state current densities for ethanol electrooxidation compared with the Pd/C electrode, indicating the higher electrocatalytic activity and durability of the $\mathrm{Pd}_{\mathrm{CD}}$ aerogels. The enhanced electrocatalytic activity of the $\mathrm{Pd}_{\alpha\text{-CD}}$ and $\mathrm{Pd}_{\beta\text{-CD}}$ aerogels relative to that of the $\mathrm{Pd}_{\gamma\text{-CD}}$ aerogel may be related to the role of these two CDs as ethanol reservoirs as a result of the size-selective host–guest interaction between the CDs and ethanol. This indicates that the left stabilizer species on the noble metal aerogels might also play an important role in improving their catalytic activity.

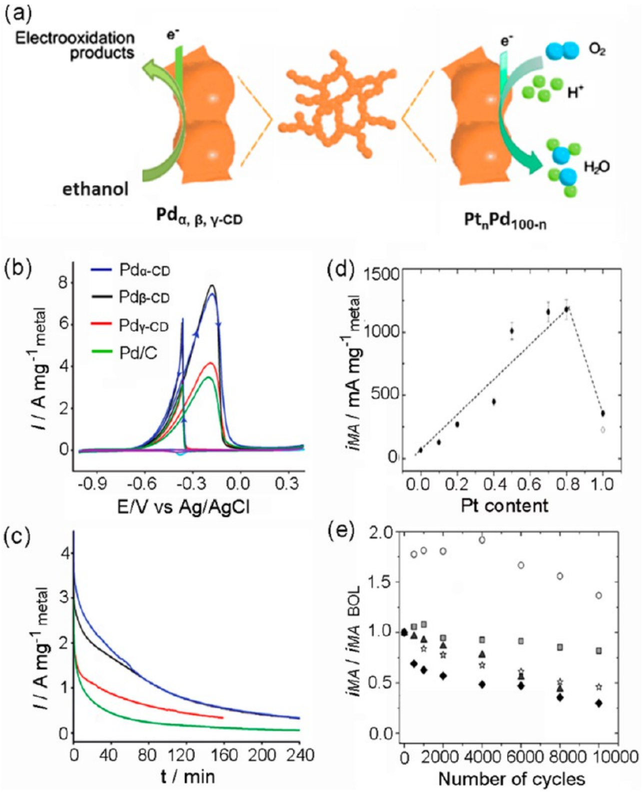

Figure 7. (a) Schematic illustration of the electrocatalytic activities of $\mathrm{Pd}_{\alpha,\beta,\gamma\text{-CD}}$ aerogels toward ethanol oxidation and $\mathrm{Pt}_n\mathrm{Pd}_{100-n}$ aerogels toward the ORR. (b) Cyclic voltammograms of electrodes modified with $\mathrm{Pd}_{\alpha,\beta,\gamma\text{-CD}}$ aerogels and Pd/C in 1.0 M KOH + 1.0 M C_2H_5OH aqueous solution. (c) Chronoamperometric curves for ethanol electrooxidation at −0.3 V/Ag/AgCl. (d) Volcano plot of the ORR mass activity of various $\mathrm{Pt}_n\mathrm{Pd}_{100-n}$ aerogel catalysts as a function of Pt content at 0.9 V vs RHE. The open circle represents the value for Pt/C. (e) Relative ORR mass activities of various $\mathrm{Pt}_n\mathrm{Pd}_{100-n}$ catalysts as functions of the number of potential cycles (linear potential sweeps between 0.5 and 1.0 V/RHE): ○, $\mathrm{Pt}_{40}\mathrm{Pd}_{60}$; ■, $\mathrm{Pt}_{80}\mathrm{Pd}_{20}$; ▲, Pt; ♦, Pd; ☆, 20% Pt/C. Panels (a–e) are reproduced with permission from refs 18 and 19. Copyright 2012 and 2013 Wiley-VCH Verlag GmbH & Co. KGaA, Weinheim.

For the ORR investigations, monometallic and bimetallic $\mathrm{Pt}_n\mathrm{Pd}_{100-n}$ aerogels generated via the in situ spontaneous gelation process were evaluated and compared with Pt/C (20 wt %).[19] The specific activity (based on the total metal loading) at 0.9 V as a function of Pt content in the aerogel shows a volcano-type behavior,[40−44] with the $\mathrm{Pt}_{80}\mathrm{Pd}_{20}$ aerogel exhibiting the highest mass-specific activity (Figure 7d). The downshift of the d-band center in the alloys, commonly used as a descriptor of the surface electronic state of ORR catalysts,[40−44] shows the same volcano-type behavior for the $\mathrm{Pt}_n\mathrm{Pd}_{100-n}$ aerogels. Therefore, the remarkable activity of the $\mathrm{Pt}_{80}\mathrm{Pd}_{20}$ aerogel indicates the best balance between the free energies of adsorption of oxygen-containing reaction species.

The comparison of the ORR activities of the Pt_nPd_{100-n} aerogels with that of Pt/C clearly indicates that Pt_nPd_{100-n} bimetallic aerogels are highly active cathode catalysts for PEFCs. The Pt_nPd_{100-n} bimetallic aerogels containing more than 40% Pt meet or even exceed the performance targets for ORR fuel cell catalysts (0.44 A mg_{Pt}^{-1} at 0.9 V vs RHE) as defined by the U.S. Department of Energy.[26] In particular the $Pt_{80}Pd_{20}$ aerogel shows the best performance and its mass activity is 5 times higher than that of the commercial Pt/C catalyst.

Durability test results (Figure 7e) indicate that the bimetallic aerogels show much better durability than the pure Pt and Pd aerogels as well as Pt/C. The commercial Pt/C catalyst and the pure Pt aerogel show similar durability with losses of 54% and 56%, respectively, after 10 000 cycles. For the $Pt_{80}Pd_{20}$ and $Pt_{40}Pd_{60}$ aerogels, the mass activity increases at the beginning and then decreases slowly, with the $Pt_{80}Pd_{20}$ aerogel having a 12% loss and the $Pt_{40}Pd_{60}$ aerogel exhibiting even a 36% increase compared with their initial mass activities. The significant enhancement of the mass activity upon potential cycling for the high-Pd-content Pt_nPd_{100-n} alloy aerogels is supposedly due to the dealloying of Pd and increased surface roughness during the potential cycling.

The higher electrocatalytic activity and durability of the Pt_nPd_{100-n} bimetallic aerogels discussed above indicate the important role of synergistic effects in their electrocatalytic applications.

The extraordinary electrocatalytic activities and durability of the Pd_{CD} aerogels toward the anodic electrooxidation of ethanol and the Pt_nPd_{100-n} aerogels toward the cathodic reduction of oxygen indicate that unsupported noble metal aerogels can be considered as a new class of very promising PEFC electrocatalysts that combine the high stability of extended surfaces with the high surface area of NPs.

■ SUMMARY AND OUTLOOK

In this Account, we have presented the design and synthetic routes of various novel noble metal aerogels and their promising applications as electrocatalysts in fuel cell cathode and anode reactions. Despite the long history of aerogels, the development of self-supported metallic aerogels and their applications are still in the early stage. A number of challenges remain before the widespread implementation of these materials in various practical areas can be realized. First, the diversity of the morphologies of the metallic aerogel is limited and needs to be enriched. This may be achieved by gelation of preformed metallic nanocrystals of different shapes or structures or by developing new strategies for gel formation. Second, the variety of the metal aerogel components is still limited, and the extension to other metal components and to desired combinations thereof is necessary. Third, although various noble metal aerogels have been successfully synthesized, great challenges still remain on how to develop general and simple strategies that can be utilized to create series of metal aerogels in scalable ways and by this reducing the aerogel cost and promoting their wide applications in practical areas. Fourth, even though a mechanism of gel formation has tentatively been proposed on the basis of the initial experiments, a detailed and in-depth understanding of the underlying processes is still missing. This unraveling is thought to be essential in order to surmount the challenges mentioned above and to achieve further breakthroughs in the development of metallic aerogels. Fifth, systematic studies of how to control the surface area and porosity of the noble metal aerogels is of great importance. Sixth, besides the effects of surface area and porosity, the surface properties of the metal (e.g., defects, exposed surface planes, and left stabilizer species) might also play important roles in their catalytic behavior, which is of great interest to study. Finally, the application of metallic aerogels is still barely explored, currently only involving the application as electrocatalysts for various electrochemical reactions or as explosives and thermites.[13] Even though these works have paved the aerogel application road, the exploration of them in fuel cell reactions in depth and width is necessary, and the applications of metallic aerogels in other areas of catalysis, other electrochemical energy systems, hydrogen storage, surface-enhanced Raman spectrocopy, sensors, etc., are of great interest and need to be explored in the near future.

■ ASSOCIATED CONTENT

Ⓢ Supporting Information

TEM monitoring of the formation of the $Pd_{\beta\text{-CD}}$ hydrogel, more detailed information on the morphologies of the noble metal aerogels including SEM and TEM images, photographs of some noble metal aerogel monoliths, SEM image of a Au−Pd xerogel film, focused ion beam (FIB) cut cross section of the Au−Ag−Pt trimetallic aerogel infiltrated with poly(ethyl cyanoacrylate), and BET surface areas of porous noble metals prepared by different techniques. This material is available free of charge via the Internet at http://pubs.acs.org.

■ AUTHOR INFORMATION

Corresponding Author

*E-mail: alexander.eychmueller@chemie.tu-dresden.de.

Present Address

#M.O.: Institute of Chemistry, Carl von Ossietzky Universität Oldenburg, Carl-von-Ossietzky Str. 9-11, D-26111 Oldenburg, Germany.

Notes

The authors declare no competing financial interest.

Biographies

Wei Liu received her Ph.D. degree (2009) from Changchun Institute of Applied Chemistry, Chinese Academy of Sciences (with Professor Xiang Gao). She worked as a Marie Curie Experienced Researcher with Professor M. Sillanpää at the University of Eastern Finland (2009−2010). Then she joined Professor Eychmüller's group at TU Dresden, first as an Alexander von Humboldt Fellow and now as a research associate. Her research interests include nanostructured metal materials and their applications in electrocatalysis, electrochemical sensors, and gas-phase heterogeneous catalysis.

Anne-Kristin Herrmann studied chemistry at TU Dresden and received her Ph.D. degree in 2014 in the group of Professor Eychmüller. Her research is focused on three-dimensional porous superstructures by self-assembly of metal nanoparticles.

Nadja C. Bigall studied physics (LMU Munich) and has conducted research in the laboratories of A. Eychmüller (TU Dresden, doctorate), T. Pellegrino and L. Manna (IIT Genoa), and W. Parak (Marburg University). Currently she works as a junior research group leader at Leibniz University Hannover, scientifically focusing on the formation of functional superstructures from nanoparticle building blocks.

Paramaconi Rodriguez obtained his Ph.D. degree in Alicante working on the electrochemical characterization of single-crystal platinum surfaces. He was a postdoctoral researcher at the University of Leiden. He continued his career as scientific officer at the Paul Scherrer Institute, and since 2012 he has been a Lecturer at the University of Birmingham (U.K.). He has published more than 40 articles in scientific journals, and his work has been recognized with awards from the International Society of Electrochemistry and the Science National Foundation of The Netherlands.

Dan Wen received her B.S. degree from Wuhan University (2006) and Ph.D. degree in analytical chemistry from Changchun Institute of Applied Chemistry, Chinese Academy of Sciences (with Professor Shaojun Dong) in 2011. She was a Humboldt Postdoctoral Fellow (2012–2014) and now is a research associate at TU Dresden. Her current research interests include synthesis, assembly, and electrocatalytic and sensing applications of nanostructured materials.

Mehtap Oezaslan received her Ph.D. degree in electrochemistry from Technische Universität Berlin, Germany in Spring 2012 (with Professor P. Strasser). In 2012–2014 she worked as scientist in the Electrochemistry Laboratory Group (Professor T. J. Schmidt) at the Paul Scherrer Institute, Switzerland. Since August 2014 she has been an Assistant Professor at Carl von Ossietzky Universität Oldenburg, focusing on electrocatalysis for fuel cells and sustainable fuel production. Her research is focused on the development and characterization of electrocatalysts for PEM fuel cells and CO_2 reduction.

Thomas J. Schmidt studied chemistry at the University of Ulm, Gemany (Ph.D. degree with R. J. Behm) and then continued his career as postdoc and scientist at Lawrence Berkeley National Laboratory (P. N. Ross and N. M. Markovic, respectively) and at Paul Scherrer Institute (PSI) (with G. G. Scherer). After eight years in industrial fuel cell research (BASF Fuel Cell) as Director of R&D, he became Chair of Electrochemistry at ETH Zürich and Head of the Electrochemistry Laboratory at PSI in 2011. His work is focused on all aspects of electrochemical energy conversion and storage.

Nikolai Gaponik received his Ph.D. degree in chemistry (2000) from the Belarusian State University. He was a visiting scientist at the LMU in Munich, a research scientist in the group of Professor H. Weller at the University of Hamburg, and an IKERBASQUE Fellow at the University of the Basque Country. He habilitated at TU Dresden in 2013, where he has been employed since 2005 as a senior scientist. His current research focuses on the assembly and applications of nanoparticles.

The academic career of **Alexander Eychmüller** started in Göttingen with studies of physics (Ph.D., MPI for Biophysical Chemistry, A. Weller and K. H. Grellmann) and continued at UCLA (postdoc with M. A. El-Sayed), Berlin (HMI with A. Henglein), and the University of Hamburg (with H. Weller). Since 2005 he has held a chair in Physical Chemistry at TU Dresden. His research interests include the synthesis and characterization of nanosized objects and their photophysical, electrochemical, and structural properties.

■ ACKNOWLEDGMENTS

Financial support from the Alexander von Humboldt Foundation, the Deutsche Forschungsgemeinschaft (Grants EY 16/10-1 and -2, RTG 1401, cfAED, and EY 16/18-1), the Swiss National Science Foundation (SNCF), and the European Research Council (ERC-2013-AdG AEROCAT) is gratefully acknowledged. N.C.B. is grateful for financial support from the German Federal Ministry of Education and Research (BMBF) within the program NanoMatFutur (support code 03X5525). We sincerely acknowledge the indispensable help of the people named in the author lines of refs 17–21, especially for their efforts in physically characterizing the gel structures.

■ REFERENCES

(1) Gesser, H. D.; Goswami, P. C. Aerogels and Related Porous Materials. *Chem. Rev.* **1989**, *89*, 765–788.

(2) Kistler, S. S. Coherent Expanded Aerogels and Jellies. *Nature* **1931**, *127*, 741–741.

(3) Hüsing, N.; Schubert, U. Aerogels—Airy Materials: Chemistry, Structure, and Properties. *Angew. Chem., Int. Ed.* **1998**, *37*, 22–45.

(4) Mahadik-Khanolkar, S.; Donthula, S.; Sotiriou-Leventis, C.; Leventis, N. Polybenzoxazine Aerogels. 1. High-Yield Room-Temperature Acid-Catalyzed Synthesis of Robust Monoliths, Oxidative Aromatization, and Conversion to Microporous Carbons. *Chem. Mater.* **2014**, *26*, 1303–1317.

(5) Leventis, N. Three-Dimensional Core–Shell Superstructures: Mechanically Strong Aerogels. *Acc. Chem. Res.* **2007**, *40*, 874–884.

(6) Mohanan, J. L.; Arachchige, I. U.; Brock, S. L. Porous Semiconductor Chalcogenide Aerogels. *Science* **2005**, *307*, 397–400.

(7) Arachchige, I. U.; Brock, S. L. Sol–Gel Methods for the Assembly of Metal Chalcogenide Quantum Dots. *Acc. Chem. Res.* **2007**, *40*, 801–809.

(8) Bag, S.; Trikalitis, P. N.; Chupas, P. J.; Armatas, G. S.; Kanatzidis, M. G. Porous Semiconducting Gels and Aerogels from Chalcogenide Clusters. *Science* **2007**, *317*, 490–493.

(9) Leventis, N.; Chandrasekaran, N.; Sotiriou-Leventis, C.; Mumtaz, A. Smelting in the Age of Nano: Iron Aerogels. *J. Mater. Chem.* **2009**, *19*, 63–65.

(10) Mulik, S.; Sotiriou-Leventis, C.; Leventis, N. Time-Efficient Acid-Catalyzed Synthesis of Resorcinol–Formaldehyde Aerogels. *Chem. Mater.* **2007**, *19*, 6138–6144.

(11) Leventis, N.; Chandrasekaran, N.; Sadekar, A. G.; Mulik, S.; Sotiriou-Leventis, C. The Effect of Compactness on the Carbothermal Conversion of Interpenetrating Metal Oxide/Resorcinol–Formaldehyde Nanoparticle Networks to Porous Metals and Carbides. *J. Mater. Chem.* **2010**, *20*, 7456–7471.

(12) Leventis, N.; Chandrasekaran, N.; Sadekar, A. G.; Sotiriou-Leventis, C.; Lu, H. One-Pot Synthesis of Interpenetrating Inorganic/Organic Networks of CuO/Resorcinol–Formaldehyde Aerogels: Nanostructured Energetic Materials. *J. Am. Chem. Soc.* **2009**, *131*, 4576–4577.

(13) Mahadik-Khanolkar, S.; Donthula, S.; Bang, A.; Wisner, C.; Sotiriou-Leventis, C.; Leventis, N. Polybenzoxazine Aerogels. 2. Interpenetrating Networks with Iron Oxide and the Carbothermal Synthesis of Highly Porous Monolithic Pure Iron(0) Aerogels as Energetic Materials. *Chem. Mater.* **2014**, *26*, 1318–1331.

(14) Tappan, B. C.; Steiner, S. A.; Luther, E. P. Nanoporous Metal Foams. *Angew. Chem., Int. Ed.* **2010**, *49*, 4544–4565.

(15) Moreno-Castilla, C.; Maldonado-Hódar, F. J. Carbon Aerogels for Catalysis Applications: An Overview. *Carbon* **2005**, *43*, 455–465.

(16) Morris, C. A.; Anderson, M. L.; Stroud, R. M.; Merzbacher, C. I.; Rolison, D. R. Silica Sol as a Nanoglue: Flexible Synthesis of Composite Aerogels. *Science* **1999**, *284*, 622–624.

(17) Bigall, N. C.; Herrmann, A.-K.; Vogel, M.; Rose, M.; Simon, P.; Carrillo-Cabrera, W.; Dorfs, D.; Kaskel, S.; Gaponik, N.; Eychmüller, A. Hydrogels and Aerogels from Noble Metal Nanoparticles. *Angew. Chem., Int. Ed.* **2009**, *48*, 9731–9734.

(18) Liu, W.; Herrmann, A.-K.; Geiger, D.; Borchardt, L.; Simon, F.; Kaskel, S.; Gaponik, N.; Eychmüller, A. High-Performance Electrocatalysis on Palladium Aerogels. *Angew. Chem., Int. Ed.* **2012**, *51*, 5743–5747.

(19) Liu, W.; Rodriguez, P.; Borchardt, L.; Foelske, A.; Yuan, J.; Herrmann, A.-K.; Geiger, D.; Zheng, Z.; Kaskel, S.; Gaponik, N.; Kötz, R.; Schmidt, T. J.; Eychmüller, A. Bimetallic Aerogels: High-Performance Electrocatalysts for the Oxygen Reduction Reaction. *Angew. Chem., Int. Ed.* **2013**, *52*, 9849–9852.

(20) Schmidt, T. J.; Rodriguez, P.; Rabis, A.; Foelske-Schmitz, A.; Kötz, R.; Eychmüller, A.; Liu, W.; Yuan, J.; Gaponik, N.; Hermann, A.-K. Hochoberflächiger Trägerloser Katalysator für Elektrochemische Prozesse und Verfahren zu Seiner Herstellung. Eur. Pat. Appl. EP 12177908, 2012.

(21) Herrmann, A.-K.; Formanek, P.; Borchardt, L.; Klose, M.; Giebeler, L.; Eckert, J.; Kaskel, S.; Gaponik, N.; Eychmüller, A. Multimetallic Aerogels by Template-Free Self-Assembly of Au, Ag, Pt, and Pd Nanoparticles. *Chem. Mater.* **2014**, *26*, 1074−1083.

(22) Ranmohotti, K. G. S.; Gao, X.; Arachchige, I. U. Salt-Mediated Self-Assembly of Metal Nanoshells into Monolithic Aerogel Frameworks. *Chem. Mater.* **2013**, *25*, 3528−3534.

(23) Gao, X.; Esteves, R. J.; Luong, T. T. H.; Jaini, R.; Arachchige, I. U. Oxidation-Induced Self-Assembly of Ag Nanoshells into Transparent and Opaque Ag Hydrogels and Aerogels. *J. Am. Chem. Soc.* **2014**, *136*, 7993−8002.

(24) Hayden, B. E. Particle Size and Support Effects in Electrocatalysis. *Acc. Chem. Res.* **2013**, *46*, 1858−1866.

(25) Perez-Alonso, F. J.; McCarthy, D. N.; Nierhoff, A.; Hernandez-Fernandez, P.; Strebel, C.; Stephens, I. E. L.; Nielsen, J. H.; Chorkendorff, I. The Effect of Size on the Oxygen Electroreduction Activity of Mass-Selected Platinum Nanoparticles. *Angew. Chem., Int. Ed.* **2012**, *51*, 4641−4643.

(26) Rabis, A.; Rodriguez, P.; Schmidt, T. J. Electrocatalysis for Polymer Electrolyte Fuel Cells: Recent Achievements and Future Challenges. *ACS Catal.* **2012**, *2*, 864−890.

(27) Debe, M. K. Electrocatalyst Approaches and Challenges for Automotive Fuel Cells. *Nature* **2012**, *486*, 43−51.

(28) Porter, N. S.; Wu, H.; Quan, Z.; Fang, J. Shape-Control and Electrocatalytic Activity-Enhancement of Pt-Based Bimetallic Nanocrystals. *Acc. Chem. Res.* **2013**, *46*, 1867−1877.

(29) Wu, J.; Yang, H. Platinum-Based Oxygen Reduction Electrocatalysts. *Acc. Chem. Res.* **2013**, *46*, 1848−1857.

(30) Cui, C.-H.; Yu, S.-H. Engineering Interface and Surface of Noble Metal Nanoparticle Nanotubes toward Enhanced Catalytic Activity for Fuel Cell Applications. *Acc. Chem. Res.* **2013**, *46*, 1427−1437.

(31) Chen, Z.; Waje, M.; Li, W.; Yan, Y. Supportless Pt and PtPd Nanotubes as Electrocatalysts for Oxygen-Reduction Reactions. *Angew. Chem., Int. Ed.* **2007**, *46*, 4060−4063.

(32) Fabbri, E.; Rabis, A.; Kötz, R.; Schmidt, T. J. Pt Nanoparticles Supported on Sb−SnO_2 Porous Structures: Developments and Issues. *Phys. Chem. Chem. Phys.* **2014**, *16*, 13672−13681.

(33) Fabbri, E.; Patru, A.; Rabis, A.; Kötz, R.; Schmidt, T. J. Advanced Cathode Materials for Polymer Electrolyte Fuel Cells Based on Pt/Metal Oxides: From Model Electrodes to Catalyst Systems. *Chimia* **2014**, *68*, 217−220.

(34) Park, J.-W.; Shumaker-Parry, J. S. Structural Study of Citrate Layers on Gold Nanoparticles: Role of Intermolecular Interactions in Stabilizing Nanoparticles. *J. Am. Chem. Soc.* **2014**, *136*, 1907−1921.

(35) Rolison, D. R. Catalytic Nanoarchitectures—The Importance of Nothing and the Unimportance of Periodicity. *Science* **2003**, *299*, 1698−1701.

(36) Leventis, N.; Sotiriou-Leventis, C.; Zhang, G.; Rawashdeh, A.-M. M. Nanoengineering Strong Silica Aerogels. *Nano Lett.* **2002**, *2*, 957−960.

(37) Gaponik, N.; Wolf, A.; Marx, R.; Lesnyak, V.; Schilling, K.; Eychmüller, A. Three-Dimensional Self-Assembly of Thiol-Capped CdTe Nanocrystals: Gels and Aerogels as Building Blocks for Nanotechnology. *Adv. Mater.* **2008**, *20*, 4257−4262.

(38) van der Pauw, L. J. A Method of Measuring Specific Resistivity and Hall Effect of Discs of Arbitrary Shapes. *Philips Res. Rep.* **1958**, *13*, 1−9.

(39) Parlett, C. M. A.; Wilson, K.; Lee, A. F. Hierarchical Porous Materials: Catalytic Applications. *Chem. Soc. Rev.* **2013**, *42*, 3876−3893.

(40) Stamenkovic, V. R.; Mun, B. S.; Arenz, M.; Mayrhofer, K. J. J.; Lucas, C. A.; Wang, G.; Ross, P. N.; Markovic, N. M. Trends in Electrocatalysis on Extended and Nanoscale Pt-Bimetallic Alloy Surfaces. *Nat. Mater.* **2007**, *6*, 241−247.

(41) Cai, Y.; Adzic, R. R. Platinum Monolayer Electrocatalysts for the Oxygen Reduction Reaction: Improvements Induced by Surface and Subsurface Modifications of Cores. *Adv. Phys. Chem.* **2011**, No. 530397.

(42) Zhang, J.; Vukmirovic, M. B.; Xu, Y.; Mavrikakis, M.; Adzic, R. R. Controlling the Catalytic Activity of Platinum-Monolayer Electrocatalysts for Oxygen Reduction with Different Substrates. *Angew. Chem., Int. Ed.* **2005**, *44*, 2132−2135.

(43) Stamenkovic, V.; Mun, B. S.; Mayrhofer, K. J. J.; Ross, P. N.; Markovic, N. M.; Rossmeisl, J.; Greeley, J.; Nørskov, J. K. Changing the Activity of Electrocatalysts for Oxygen Reduction by Tuning the Surface Electronic Structure. *Angew. Chem., Int. Ed.* **2006**, *45*, 2897−2901.

(44) Viswanathan, V.; Hansen, H. A.; Rossmeisl, J.; Nørskov, J. K. Universality in Oxygen Reduction Electrocatalysis on Metal Surfaces. *ACS Catal.* **2012**, *2*, 1654−1660.